Difference in the sensitivity to cytokine stimulations in different species may even play a role in the pathogenesis of hantavirus infections. Hantaviruses are pathogenic to humans but not to the natural hosts, rodents, except for suckling animals [30, 34, 38, 44]. It is, therefore, tempting to postulate that the high sensitivity of human to pro-inflammatory cytokines [10] may be one of the possible explanations for the different pathogenesis between human and other animals, assuming that the combination of the low level of TNF-alpha and the endothelial cell infection plays a major role in the pathogenesis of human hantavirus infections.

Acknowledgements

We thank Ms. M. Ogata for her assistance and Dr. J. Arikawa for helpful discussion and providing HTNV. This study was supported by grants from the Ministry of Health, Welfare, and Labor and the Ministry of Education, Science, Culture and Sports of Japan.

References

1. Anderson R, Wang S, Osiowy C, Issekutz AC (1997) Activation of endothelial cells via antibody-enhanced dengue virus infection of peripheral blood monocytes. J Virol 71: 4226–4232
2. Blum MS, Toninelli E, Anderson JM, Balda MS, Zhou J, O'Donnell L, Pardi R, Bender JR (1997) Cytoskeletal rearrangement mediates human microvascular endothelial tight junction modulation by cytokines. Am J Physiol 273: H286–H294
3. Bonner SM, O'Sullivan MA (1998) Endothelial cell monolayers as a model system to investigate dengue shock syndrome. J Virol Methods 71: 159–167
4. Bove K, Neumann P, Gertzberg N, Johnson A (2001) Role of ecNOS-derived NO in mediating TNF-induced endothelial barrier dysfunction. Am J Physiol-Lung Cell Mol Physiol 280: L914–L922
5. Brett J, Gerlach H, Nawroth P, Steinberg S, Godman G, Stern D (1989) Tumor necrosis factor/cachectin increases permeability of endothelial cell monolayers by a mechanism involving regulatory G proteins. J Exp Med 169: 1977–1991
6. Butler JC, Peters CJ (1994) Hantaviruses and hantavirus pulmonary syndrome. Clin Infect Dis 19: 387–394
7. Cosgriff TM (1991) Mechanisms of disease in hantavirus infection: pathophysiology of hemorrhagic fever with renal syndrome. Rev Infect Dis 13: 97–107
8. De Assis MC, Da Casta AO, Barja-Fidalgo TC, Plotkowski MC (2000) Human endothelial cells are activated by interferon-gamma plus tumor necrosis factor-alpha to kill intracellular *Pseudomonas aeroginosa.* Immunology 101: 271–278
9. Davis IC, Zajac AJ, Nolte KB, Botten J, Hjelle B, Matalon S (2002) Elevated generation of reactive oxygen/nitrogen species in hantavirus cardiopulmonary syndrome. J Virol 76: 8347–8359
10. Dinarello CA (1996) Cytokines as mediators in the pathogenesis of septic shock. Curr Topic Microbiol Immunol 216: 133–165
11. Fisher-Hoch SP, Platt GS, Neild GH, Southee T, Baskerville A, Raymond G, Lloyd RT, Simpson DI (1985) Pathophysiology of shock and hemorrhage in a fulminating viral infection (Ebola). J Infect Dis 152: 887–894
12. Freyer D, Manz R, Ziegenhorn A, Weih M, Angstwurm K, Docke WD, Meisel A, Schumann RR, Schonfelder G, Dirnagl U, Weber JR (1999) Cerebral endothelial cells release TNF-alpha after stimulation with cell walls of *Streptococcus pneumoniae* and

regulate inducible nitric oxide synthase and ICAM-1 expression via autocrine loops. J Immunol 163: 4308–4314
13. Geimonen E, Neff S, Raymond T, Kocer SS, Gavrilovskaya IN, Mackow ER (2002) Pathogenic and nonpathogenic hantavuris differently regulate endothelial cell responses. Proc Natl Acad Sci USA 99: 13837–13842
14. Goldblum SE, Sun WL (1990) Tumor necrosis factor-alpha augments pulmonary arterial transendothelial albumin flux in vitro. Am J Physiol 258: L57–L67
15. Griffith OW, Kilbourn RG (1996) Nitric oxide synthase inhibitors: Amino acids. In: Packer L (ed) Nitric oxide part A. Methods in enzymology *268*. Academic Press, New York, pp. 375–392
16. Kang JI, Park SH, Lee PW, Ahn BY (1999) Apoptosis is induced by hantaviruses in cultured cells. Virology 264: 99–105
17. Khaiboullina SF, Netski DM, Krumpe P, St Jeor SC (2000) Effects of tumor necrosis factor alpha on Sin Nombre virus infection *in vitro*. J Virol 74: 11966–11971
18. Kim GR, McKee KT Jr (1985) Pathogenesis of Hantaan virus infection in suckling mice: clinical, virologic, and serologic observations. Am J Trop Med Hyg 34: 388–395
19. Klingstrom J, Plyusnin A, Vaheri A, Lundkvist A (2002) Wild-type Puumala hantavirus infection induces cytokines, C-reactive protein, creatinine, and nitric oxide in cynomolgus macaques. J Virol 76: 444–449
20. Lampugnani MG, Corada M, Caveda L, Breviario F, Ayalon O, Geiger B, Dejana E (1995) The molecular organization of endothelial cell to cell junctions: differential association of plakoglobin, beta-catenin, and alpha-catenin with vascular endothelial cadherin (VE-cadherin). J Cell Biol 129: 203–217
21. Linderholm M, Billstrom A, Settergren B, Tarnvik A (1992) Pulmonary involvement in nephropathia epidemica as demonstrated by computed tomography. Infection 20: 263–266
22. Linderholm M, Ahlm C, Settergren B, Waage A, Tarnvik A (1996) Elevated plasma levels of tumor necrosis factor (TNF)-alpha, soluble TNF receptors, interleukin (IL)-6, and IL-10 in patients with hemorrhagic fever with renal syndrome. J Infect Dis 173: 38–43
23. Linderholm M, Groeneveld PH, Tarnvik A (1996) Increased production of nitric oxide in patients with hemorrhagic fever with renal syndrome – relation to arterial hypotension and tumor necrosis factor. Infection 24: 337–340.
24. Lukes RJ (1954) The pathology of thirty-nine fatal cases of epidemic hemorrhagic fever. Am J Pathol 16: 639–650
25. Mackay F, Loetscher H, Stueber D, Gehr G, Lesslauer W (1993) Tumor necrosis factor α (TNF-α)-induced cell adhesion to human endothelial cells is under dominant control of one TNF receptor type, TNF-R55. J Exp Med 177: 1277–1286
26. Mantovani A, Bussolino F, Dejana, E (1992) Cytokine regulation of endothelial cell function. FASEB J 6: 2591–2599
27. Mantovani A, Bussolino F, Introna M (1997) Cytokine regulation of endothelial cell function: from molecular level to the bedside. Immunol Today 18: 231–240
28. Mark KS, Trickler WJ, Miller DW (2001) Tumor necrosis factor-alpha induces cyclooxygenase-2 expression and prostaglandin release in brain microvessel endothelial cells. J Pharmacol Exp Ther 297: 1051–1058
29. Maruo N, Morita I, Shirao M, Murota S (1992) IL-6 increases endothelial permeability in vitro. Endocrinology 131: 710–714
30. McKee KT Jr, Kim GR, Green DE, Peters CJ (1985) Hantaan virus infection in suckling mice: virologic and pathologic correlates. J Med Virol 17: 107–117

31. Meyer BJ, Schmaljohn CS (2000) Persistent hantavirus infections: characteristics and mechanisms. Trend Microbiol 8: 61–67
32. Mori M, Rothman AL, Kurane I, Montoya JM, Nolte KB, Norman JE, Waite DC, Koster FT, Ennis FA (1999) High levels of cytokine-producing cells in the lung tissues of patients with fatal hantavirus pulmonary syndrome. J Infect Dis 179: 295–302
33. Munro JM, Pober JS, Cotran RS (1989) Tumor necrosis factor and interferon-gamma induce distinct patterns of endothelial activation and associated leukocyte accumulation in skin of Papio anubis. Am J Pathol 135: 121–133
34. Nakamura T, Yanagihara R, Gibbs CJ Jr, Amyx HL, Gajdusek DC (1985) Differential susceptibility and resistance of immunocompetent and immunodeficient mice to fatal Hantaan virus infection. Arch Virol 86: 109–120
35. Nolte KB, Feddersen RM, Foucar K, Zaki SR, Koster FT, Madar D, Merlin TL, McFeeley PJ, Umland ET, Zumwalt RE (1995) Hantavirus pulmonary syndrome in the United States: a pathological description of a disease caused by a new agent. Human Pathol 26: 110–120
36. Pensiero MN, Sharefkin JB, Dieffenbach CW, Hay J (1992) Hantaan virus infection of human endothelial cells. J Virol 66: 5929–5936
37. Peters CJ, Khan AS (2002) Hantavirus pulmonary syndrome: The New American hemorrhagic fever. Clin Infect Dis 34: 1224–1231
38. Plyusnin A, Vapalahti O, Vaheri A (1996) Hantaviruses: genome structure, expression and evolution. J Gen Virol 77: 2677–2687
39. Raftery MJ, Kraus AA, Ulrich R, Kruger DH, Schonrich G (2002) Hantavirus infection of dendritic cells. J Virol 76: 10724–10733
40. Royall JA, Berkow RL, Beckman JS, Cunningham MK, Matalon S, Freeman BA (1989) Tumor necrosis factor and interleukin 1 alpha increase vascular endothelial permeability. Am J Physiol-Lung Cell Mol Physiol 257: L399–L410
41. Sugiyama K, Morikawa S, Matsuura Y, Tkachenko EA, Morita C, Komatsu T, Akao Y, Kitamura T (1987) Four serotypes of haemorrhagic fever with renal syndrome viruses identified by polyclonal and monoclonal antibodies. J Gen Virol 68: 979–987
42. Sundstrom JB, McMullan LK, Spiropoulou CF, Hooper WC, Ansari AA, Peters CJ, Rollin PE (2001) Hantavirus infection induces the expression of RANTES and IP-10 without causing increased permeability in human lung microvascular endothelial cells. J Virol 75: 6070–6085.
43. Yanagihara R, Silverman DJ (1990) Experimental infection of human vascular endothelial cells by pathogenic and nonpathogenic hantaviruses. Arch Virol 111: 281–286
44. Yoshimatsu K, Arikawa J, Ohbora S, Itakura C (1997) Hantavirus infection in SCID mice. J Vet Med Sci 59: 863–868
45. Zaki SR, Greer PW, Coffield LM, Goldsmith CS, Nolte KB, Foucar K, Feddersen RM, Zumwalt RE, Miller GL, Khan AS, Rollin PE, Ksiazek TG, Nicole ST, Mahy BWJ, Peters CJ (1995) Hantavirus pulmonary syndrome. Pathogenesis of an emerging infectious disease. Am J Pathol 146: 552-579

Author's address: Shigeru Morikawa, DVM, Ph.D., 4-7-1 Gakuen, Musashimurayam, 208–0011 Tokyo, Japan; e-mail: morikawa@nih.go.jp

International Immunology Advance Access published August 16, 2004

International Immunology 2004; 1 of 8
doi:10.1093/intimm/dxh143

A subcutaneously injected UV-inactivated SARS coronavirus vaccine elicits systemic humoral immunity in mice

Naomi Takasuka[1], Hideki Fujii[1], Yoshimasa Takahashi[1], Masataka Kasai[1], Shigeru Morikawa[2], Shigeyuki Itamura[4], Koji Ishii[3], Masahiro Sakaguchi[1], Kazuo Ohnishi[1], Masamichi Ohshima[1], Shu-ichi Hashimoto[1], Takato Odagiri[4], Masato Tashiro[4], Hiroshi Yoshikura[5], Toshitada Takemori[1] and **Yasuko Tsunetsugu-Yokota[1]**

[1]Department of Immunology, [2]First, [3]Second and [4]Third Departments of Virology, [5]National Institute of Infectious Diseases, Toyama 1-23-1, Shinjuku-ku, Tokyo 162-8640, Japan

Keywords: alum, cellular immunity, neutralizing antibody, parenteral administration, vaccination

Abstract

The recent emergence of severe acute respiratory syndrome (SARS) was caused by a novel *coronavirus*, SARS-CoV. It spread rapidly to many countries and developing a SARS vaccine is now urgently required. In order to study the immunogenicity of UV-inactivated purified SARS-CoV virion as a vaccine candidate, we subcutaneously immunized mice with UV-inactivated SARS-CoV with or without an adjuvant. We chose aluminum hydroxide gel (alum) as an adjuvant, because of its long safety history for human use. We observed that the UV-inactivated SARS-CoV virion elicited a high level of humoral immunity, resulting in the generation of long-term antibody secreting and memory B cells. With the addition of alum to the vaccine formula, serum IgG production was augmented and reached a level similar to that found in hyper-immunized mice, though it was still insufficient to elicit serum IgA antibodies. Notably, the SARS-CoV virion itself was able to induce long-term antibody production even without an adjuvant. Anti-SARS-CoV antibodies elicited in mice recognized both the spike and nucleocapsid proteins of the virus and were able to neutralize the virus. Furthermore, the UV-inactivated virion induced regional lymph node T-cell proliferation and significant levels of cytokine production (IL-2, IL-4, IL-5, IFN-γ and TNF-α) upon restimulation with inactivated SARS-CoV virion *in vitro*. Thus, a whole killed virion could serve as a candidate antigen for a SARS vaccine to elicit both humoral and cellular immunity.

Introduction

A new disease called severe acute respiratory syndrome (SARS) originated in China in late 2002 and spread rapidly to many countries. Upon this outbreak, a global collaboration network was coordinated by WHO. As a result of this unprecedented international effort, a novel type of coronavirus (SARS-CoV) was identified as the etiologic agent of SARS (1,2) in March 2003. The genomic sequence of SARS-CoV was completed and we now know that SARS-CoV has all the features and characteristics of other coronaviruses, but it is quite different from all previously known coronaviruses (groups I~III), representing a new group (group IV) (3,4). It is assumed that SARS-CoV is a mutant coronavirus transmitted from a wild animal that developed the ability to productively infect humans (3,5). The genome of SARS-CoV is a single-stranded plus-sense RNA ~30 kb in length and containing five major open reading frames that encode nonstructural replicase polyproteins and structural proteins: the spike (S), envelope (E), membrane (M) and nucleocapsid protein (N), in the same order and of approximately the same sizes as those of other coronaviruses (5).

The reason why SARS-CoV induces severe respiratory distress in some, but not all, infected individuals is still unclear. In patients with SARS and probable SARS cases, virus is detected in sputum, stool and plasma by RT-PCR (1,2). These patients developed serum antibodies against SARS-CoV and high antibody titers against N protein were maintained for more than 5 months after infection (6). Because of their generally poor pathogenicity and difficulty of propagation

Correspondence to: Y. Tsunetsugu-Yokota; E-mail: yyokota@nih.go.jp

Transmitting editor: K. Sugamura

Received 6 May 2004, *accepted* 15 July 2004

in vitro, there have been few studies regarding immunity to human coronaviruses OC43 and 229E. In the veterinary field, however, coronaviruses have been known for many years to cause a variety of lung, liver and gut diseases in animals. As we learned from these animal models, both humoral and cellular immune responses may contribute to protection against coronavirus diseases, including SARS [for review see (7)].

The clinical manifestation of SARS is hardly distinct from other common respiratory viral infections including influenza. Because an influenza epidemic may occur simultaneously with the re-emergence of SARS, it is urgently required that we develop effective SARS vaccines as well as sensitive diagnostic tests specific for SARS. Recently, the angiotensin-converting enzyme 2 (ACE2) was identified as a cellular receptor for SARS-CoV (8). The first step in viral infection is presumably the binding of S protein to its receptor, ACE2. In the murine MHV model, S proteins are known to contain important virus-neutralizing epitopes that elicit neutralizing antibodies in mice (9,10). Therefore, the S protein would be the first candidate coronavirus protein for induction of immunity. However, the S, M and N proteins are also known to contribute to generating the host immune response (11,12).

Following an established vaccine protocol is one of the best ways to shorten the time and cost of new vaccine development. Most of the currently available vaccines for humans are inactivated and applied cutaneously, except oral polio vaccine, and adjuvant usage is mostly limited to aluminum hydroxide gel (alum). In order to know the immunogenicity of inactivated SARS-CoV as a vaccine candidate, we immunized mice with UV-inactivated SARS-CoV either with or without alum. We report here the evaluation of humoral and cellular immunity elicited by UV-inactivated SARS-CoV administered subcutaneously.

Methods

Preparation of UV-inactivated purified SARS-CoV

SARS-CoV (HKU39849) was kindly supplied by Dr J.S.M. Peiris, Department of Microbiology, The University of Hong Kong. The virus was amplified in Vero E6 cells and purified by sucrose density gradient centrifugation. Concentrated virus was then exposed to UV light (4.75 J/cm^2) in order to inactivate the virus. We confirmed that the virus completely lost its infectivity by this method.

Immunization of mice

Female BALB/c mice were purchased from Nippon SLC Inc. (Shizuoka, Japan) and were housed under specific pathogen-free conditions. All experimental procedures were carried out under NIID-recommended guidelines. Mice were subcutaneously injected via their back or right and left hind leg footpads with 10 μg of UV-inactivated purified SARS-CoV with or without 2 mg of alum, and boosted by the same procedure 7 weeks after priming.

Detection of immunoglobulins in the serum samples

Blood was obtained from the tail vein and allowed to clot overnight at 4°C. Sera were then collected by centrifugation. For ELISA, microtiter plates (Dynatech, Chantily, VA) were coated overnight at 4°C with SARS-CoV-infected or mock-infected Vero E6 cell lysates, which had been treated with 1% NP40 followed by UV-inactivation. To detect S or N protein, the plates were coated with 1% NP40 lysates of chick embryo fibroblasts that had been infected with S or N protein-expressing DIs (attenuated vaccinia virus) (13). The plates were blocked with 1% OVA in PBS–Tween (0.05%) and then incubated with the sera serially diluted at 1:25–1:10^5 for 1 h at room temperature. Plates were incubated with either peroxidase-conjugated anti-mouse IgG (1:2000, Zymed, San Francisco, CA), IgM or IgA (1:2000, Southern Biotechnology, Birmingham, AL) antibody. For detection of IgG subclasses, either peroxidase-conjugated anti-mouse IgG_1, IgG_{2a}, IgG_{2b} (1:2000, Zymed) or IgG_3 (1:2000, Southern Biotechnology) was used. Plates were washed three times with PBS–Tween at each step. Antibodies were detected by *O*-phenylenediamine (Zymed), and the absorbance of each well was read at 490 nm using a model 680 microplate reader (Bio-Rad, Hercules, CA). As a standard for IgG detection, serum was obtained from a hyper-immunized mouse; the OD490nm value of 100 U/ml standard was ~3 in all assays. SARS-CoV-specific IgG titer was calculated as follows: SARS-specific IgG titer (U/ml) = (the unit value obtained at wells coated with virus-infected cell lysates) – (the unit value obtained at wells coated with non-infected cell lysates).

ELISPOT assay for antibody-secreting cells (ASCs)

Recombinant N protein (amino acids 1–49 and 340–390) of SARS-CoV (Biodesign, Saco, ME) was diluted to 10 μg/ml in PBS, and then added at 100 μl per well to plates supported by a nitrocellulose filter (Millipore, Bedford, MA). After overnight incubation at 4°C, the plates were washed with PBS three times and then blocked at 4°C overnight with 1% OVA in PBS–Tween (0.05%). After erythrocyte lysis, single cell suspensions from BMs were suspended in RPMI supplemented with 10% FCS, 5 × 10^{-5} M 2ME, 2 mM L-glutamine, 100 U/ml penicillin and 100 μg/ml streptomycin, and then applied to the plates at a concentration of 3 × 10^5 cells per well. After 24 h cultivation, the plates were recovered and stained with alkaline phosphatase-conjugated anti-mouse IgG_1 antibody (Southern Biotechnologies). Alkaline phosphatase activity was visualized using 3-amino-ethyl carbozole and napthol AS-MX phosphate/fast blue BB (Sigma). The frequency of plasma cells specific for N protein was determined from the N protein-coated plates after background on the uncoated plates was subtracted.

Coronavirus neutralizing assay

Serum was inactivated by incubation at 56°C for 30 min. The known tissue culture infectious dose (TCID) of SARS-CoV was incubated for 1 h in the presence or absence of serum antibodies serially diluted 5-fold, and then added to Vero E6 cell culture grown confluently in a 96-well microtiter plate. After 48 h, cells were fixed with 10% formaldehyde and stained with crystal violet to visualize the cytopathic effect induced by the virus (14). Neutralization antibody titers were expressed as the minimum dilution number of serum that inhibited the cytopathic effect.

Western blotting

Purified SARS-CoV virion (0.5 μg) was fractionated on SDS-PAGE under reduced conditions. Proteins were transferred to PVDF membrane (Genetics, Tokyo, Japan) and reacted with the diluted sera (1:1000) that had been obtained from mice inoculated with UV-irradiated SARS-CoV. After washing, the membrane was reacted with HRP-conjugated $F(ab')_2$ fragment anti-mouse IgG (H+L) (1:20 000 Jackson Immuno Research, West Grove, PA), followed by visualization of the bands on X-ray film (Kodak, Rochester, NY) using chemiluminescent regents (Amasham Biosciences, Piscataway, NJ).

Regional T cell response

Popliteal and inguinal lymph nodes and spleens were harvested from mice 1 week after the boost vaccination. After the preparation of a single cell suspension, T cells were purified by depletion of $B220^+$, $Gr1^+$, $CD11b^+$, IgD^+ and IgM^+ cells using a magnetic cell sort system (MACS: Miltenyi Biotec, Bergisch Gladbach, Germany). To prepare antigen-presenting cells (APC), normal BALB/c mouse splenocytes were depleted of $CD3^+$ T cells by MACS and irradiated at 2000 cGy.

Purified T cells taken from lymph nodes (1×10^5 cells/well) were cultured with irradiated APC (5×10^5 cells/well) in the presence or absence of UV-irradiated purified SARS-CoV virion (1 or 10 μg/ml). Four days after the cultivation, the level of cytokine concentration in the culture supernatant was measured by flow cytometry using a mouse Th1/Th2 cytokine cytometric bead array kit (Becton Dickinson, San Jose, CA). T-cell proliferation was monitored by the incorporation of [^{3}H]thymidine (18.5 kBq/well, ICN Biomedicals, Costa Mesa, CA) added 8 h prior to cell harvest. The cells were harvested on a 96-well microplate bonded with a GF/B filter (Packard Instruments, Meriden, CT). Incorporated radioactivity was counted by a microplate scintillation counter (Packard Instruments).

Results

Inoculation with UV-inactivated SARS-CoV results in an antigen-specific IgG_1 response, probably by generating long-term ASCs as well as memory cells

To examine the level of anti-SARS-CoV response in mice after inoculation with vaccine candidates, three mice in each group were subcutaneously inoculated with 10 μg of UV-inactivated purified SARS-CoV with (Virion/Alum) or without alum (Virion), or inoculated with alum alone (Alum) or left untreated (None) as a control (Fig. 1). One month after inoculation, vaccinated mice elicited the anti-SARS CoV IgG antibody in sera at high levels. As expected, the alum adjuvant enhanced the level of IgG antibody response, >10-fold higher than the level without adjuvant (Fig. 1C compared with B). When mice were boosted at 7 weeks, the level of IgG antibody in both groups of mice was further increased ~10-fold above the primary response (Fig. 1B and C). Notably, the level of serum antibodies induced by a single injection of virion, even in the absence of the alum adjuvant, was maintained at least more than 6 months (Fig. 1D). These results suggest that long-term ASCs can be established by a single shot of UV-inactivated virion administration.

Upon restimulation with antigen, memory B cells rapidly differentiate into ASCs and migrate into the bone marrow to establish a long-term ASC pool (15,16). To enumerate the number of plasma cells specific for SARS-CoV, we performed an ELISPOT assay using recombinant N proteins, amino acid numbers 1–49 (N1–49) and 340–390 (N340–390) as coating antigens. Consistent with the serum anti-SARS CoV IgG level, SARS-specific IgG_1 plasma cells were maintained in the bone marrow at day 10 after boost immunization with virion/alum

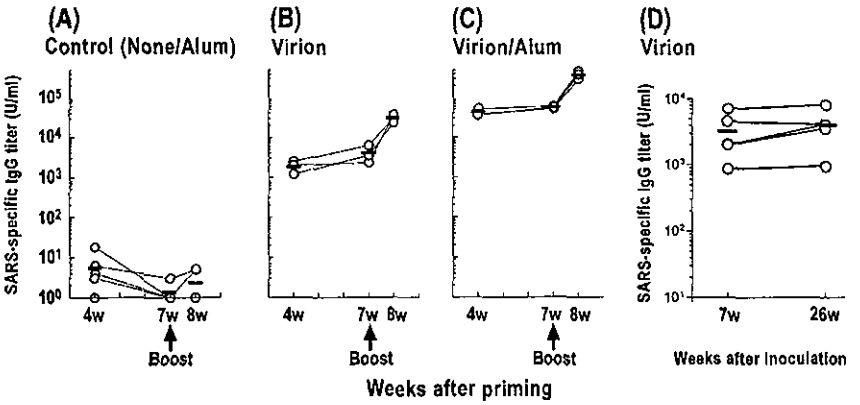

Fig. 1. The level of SARS-specific IgG in subcutaneously vaccinated mice. Mice were subcutaneously primed with 10 μg of UV-inactivated SARS-CoV virion (B), or virion with 2 mg of alum (C), or alum alone or none (A) and boosted with the same dose in their footpads at 7 weeks after priming. Serum was collected at the indicated time point and subjected to ELISA to detect SARS-specific IgG using SARS-CoV-infected Vero cell lysates as a coating antigen. Circles and bars represent the amount of IgG antibody in the serum of each mouse and the mean, respectively. The amount of IgG was arbitrarily calculated based on the concentration of hyper-immune sera. A representative result of two independent experiments is shown. (D) Mice were vaccinated with 10 μg of UV-inactivated SARS-CoV virion subcutaneously into their backs. Serum was collected from individual mice at the indicated time point and subjected to ELISA to detect SARS-specific IgG.

(Fig. 2). In contrast, the number of spots from control mice was below the detection limit (i.e. <1 ASC/9 × 10^5 cells).

UV-inactivated SARS-CoV induces IgG_1 antibody with neutralizing activity

We determined the subclass of serum anti-SARS-CoV IgG antibodies in the boosted mice using anti-mouse IgG_1, IgG_{2a}, IgG_{2b} or IgG_3 second antibody by ELISA (Fig. 3). Interestingly, the level of anti-SARS-CoV IgG_{2a} in mice immunized with virion/alum was comparable to that in mice immunized with virion alone, whereas the level of anti-SARS-CoV IgG_1 was higher in mice with virion/alum than the mice with virion alone. In contrast, the levels of IgG_{2b} and IgG_3 antibodies were fairly low in both groups. Therefore, our results indicated that vaccination with a combination of inactivated virion and alum induced a predominantly Th2-type immune response.

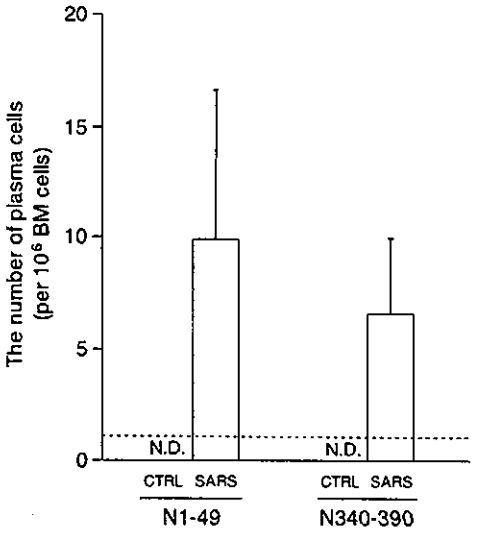

Fig. 2. The number of SARS-specific IgG_1 plasma cells in BM. Mice were primed and boosted by subcutaneous injection into their back with 10 μg of UV-inactivated SARS-CoV virion with 2 mg of alum (VA). BMs were collected at 10 days after boost and subjected to ELISPOT to detect SARS-specific IgG_1 plasma cells. Bars represent the number of plasma cells specific to N1–49 and N340–390 antigen in SARS-vaccinated and control mice, respectively. Data are means of triplicate cultures. The number of spots from control mice was below the detection limit (i.e. <1 ASC/9 × 10^5 cells: dashed line). A representative result of two independent experiments is shown. N.D.: not detected.

We also measured serum immunoglobulins other than IgG in the early and late phases of immunization. To avoid high IgG concentrations interfering with the detection of IgM and IgA antibodies, the serum IgG was absorbed with protein G-conjugated beads (>98%). The levels of anti-SARS-CoV IgM antibodies in the IgG-depleted sera, which were obtained 4 weeks after priming, were below our detection limit. Likewise, anti-SARS-CoV IgA antibody in the IgG-depleted sera, which were obtained 1 week after booster, was not detectable (data not shown).

Whether or not immune sera possess a neutralizing activity against SARS-CoV is a crucial aspect of vaccination. We estimated the neutralizing activity of sera obtained 1 week after boost inoculation (Table 1). We observed that neutralizing activity against SARS-CoV was detected at a high level in sera of mice inoculated with virion/alum or virion alone. Taken together, these results indicate that subcutaneous vaccination with UV-inactivated SARS-CoV virion is able to elicit a sufficient amount of IgG antibodies with neutralizing activity.

UV-inactivated SARS-CoV induces serum IgG antibody specific for S and N proteins

Using the immune sera of mice boosted with virion/alum 1 week before, we analyzed the specificity of serum IgG by western blot analysis (see Methods). As shown in Fig. 4(A), the robust signal detected at 50 kDa corresponds to the N protein of SARS-CoV, as predicted by its genome size (3,4). A band near 200 kDa appears to correspond to S protein, analogous with the S protein of other human coronaviruses, HCV-229E

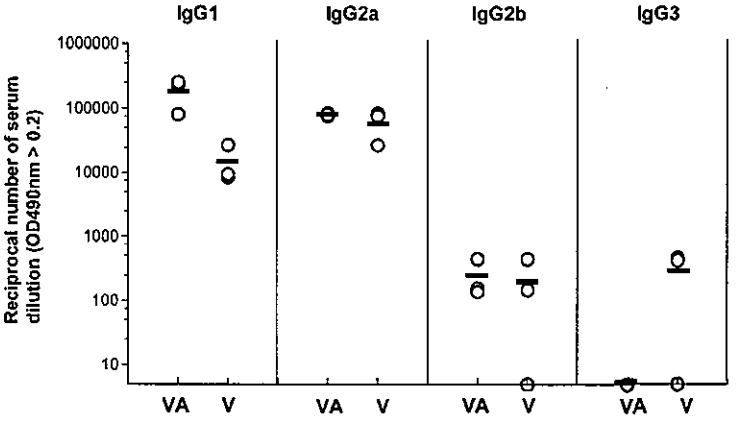

Fig. 3. IgG subclass of immunized serum. Mice were subcutaneously primed and boosted by injection in their footpads with 10 μg of UV-inactivated SARS-CoV virion (V), or virion with 2 mg of alum (VA). Serum was collected from individual mice at 1 week after boost and subjected to ELISA to detect SARS-specific IgG_1, IgG_{2a}, IgG_{2b} and IgG_3 titer. The Y value is the reciprocal serum dilution number where the OD490nm ≧ 0.2 in each ELISA. Circles and bars represent the titer for each mouse and the mean, respectively; results are representative of two separate experiments.

and HCV-OC43, which are known to be heavily glycosylated and detected at 186 kDa and 190 kDa, respectively (17). Our result is consistent with the data reported recently by Xiao *et al.* who expressed the full-length S glycoprotein of SARS-CoV Tor2 strain in 293 cells and showed that the protein ran ~180–200 kDa in SDS gels (18). The origins of the 120 kDa and the faint 37 kDa bands were unknown. However, similar bands were also detected on a fluorogram by using anti-N mAbs (Ohnishi, K., Sakaguchi, M., Takasuka, N. *et al.*, unpublished data), suggesting that it is related to N protein. The specificity of IgG in the immune sera was also determined by ELISA plates coated with lysates of cells infected with either S- or N-expressing recombinant vaccinia viruses (Fig. 4B). The results indicated that anti-S as well as anti-N protein IgG antibodies were elicited by virion/alum vaccination.

Table I. Neutralizing activity in serum after vaccination

		Reciprocal endpoint titer	
		Experiment 1	Experiment 2
None/alum		<5*	<5*
Virion	mouse 1	250	250
	2	1250	250
	3	1250	250
Virion/alum	1	250	1250
	2	1250	1250
	3	1250	1250

*All six mice examined did not have detectable neutralizing activity. Sera were obtained from mice 1 week after boost vaccination and subjected to SARS-CoV neutralizing activity assay as described in Methods. The titer is a reciprocal number of minimum serum dilution that inhibits the cytopathic effect.

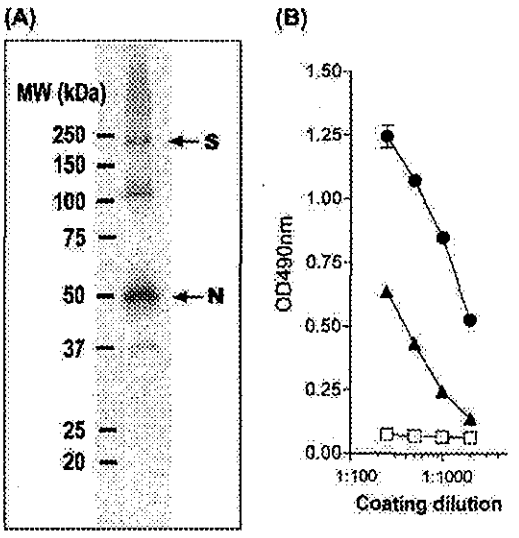

Fig. 4. Specificity of the serum antibodies. (A) Purified UV-inactivated SARS-CoV virion (0.5 μg) was fractionated by SDS–PAGE and subjected to western blotting. Diluted pooled sera (1:1000) from mice primed and boosted with virion/alum were exploited to detect virus proteins. Upper and lower arrows indicate the predicted band of S (spike protein) and N (nucleocapside protein) of SARS-CoV, respectively. The size of molecular weight markers (kDa) is shown on the left. (B) S protein- or N protein-specific ELISA. ELISA plates were coated at the indicated dilution with 1% NP40 lysates of chick embryo fibroblasts that had been infected with S protein-expressing vaccinia virus (circle), N protein-expressing vaccinia virus (triangle) or uninfected (mock; square). Diluted serum (1:1000) from mice prime and boost immunized with virion/alum, was exploited for detection of virus proteins.

UV-inactivated SARS-CoV whole virion induces T-cell response

To examine whether or not subcutaneously vaccinated mice gained an induced T-cell response against SARS-CoV, mice were immunized either with virion/alum, virion, or alum only via the footpad. T cells of these mice were enriched from the spleen and regional lymph nodes 1 week after a booster immunization and cultured with irradiated APCs in the presence or absence of UV-inactivated SARS-CoV virion at 1 or 10 μg/ml. As shown in Fig. 5(A), regional lymph node T cells proliferated *in vitro* in response to UV-inactivated virion in virion/alum-immunized mice and, to a lesser extent, in virion-immunized mice. Because mice inoculated with virion/alum showed a high basal level of proliferation of lymph node T cells in the absence of antigen, there is not much difference in the net proliferative response of these cells between the virion/alum group and the virion only group. On the other hand, in splenic T cells, a low level of proliferation was observed only in the virion/alum group of mice. The level of proliferation of these T cells, however, was virion-dose independent. Therefore, our results suggest that the subcutaneous injection of inactivated virion, even without alum, does induce T cell activation to some extent in the draining lymph node, a result which hardly occurs systemically.

We also measured the level of cytokine production in the supernatant of lymph node T cells stimulated with inactivated virion *in vitro* for 4 days. We found that the inactivated virion induced the production of all the cytokines (IL-2, IL-4, IL-5, IFN-γ and TNF-α) in T cells of virion/alum-immunized mice, in a dose-dependent manner (Fig. 5B). Likewise, T cells of virion-immunized mice produced low, yet significant, levels of these cytokines in a dose-dependent manner, except IL-5. In contrast, lymph node T cells from normal mice did not produce any cytokines at all in response to virion, suggesting that the virion itself does not possess innate stimulating activity as bacterial products [such as lipopolysaccharide (LPS) and purified protein derivative of mycobacterium tuberculosis (PPD)] do. Taken together, these results suggest that subcutaneous vaccination with UV-inactivated SARS-CoV is able to activate $CD4^+$ T cells in regional lymph nodes, where T cells produce several immunoregulatory cytokines, including IFN-γ.

Discussion

The present results demonstrated that even a single subcutaneous administration of UV-irradiated virion without alum adjuvant induced a high level of systemic anti-SARS-CoV antibody response in mice, probably followed by the generation of long-term antibody-secreting cells and memory cells in the bone marrow. Considering that polyvalent particulate

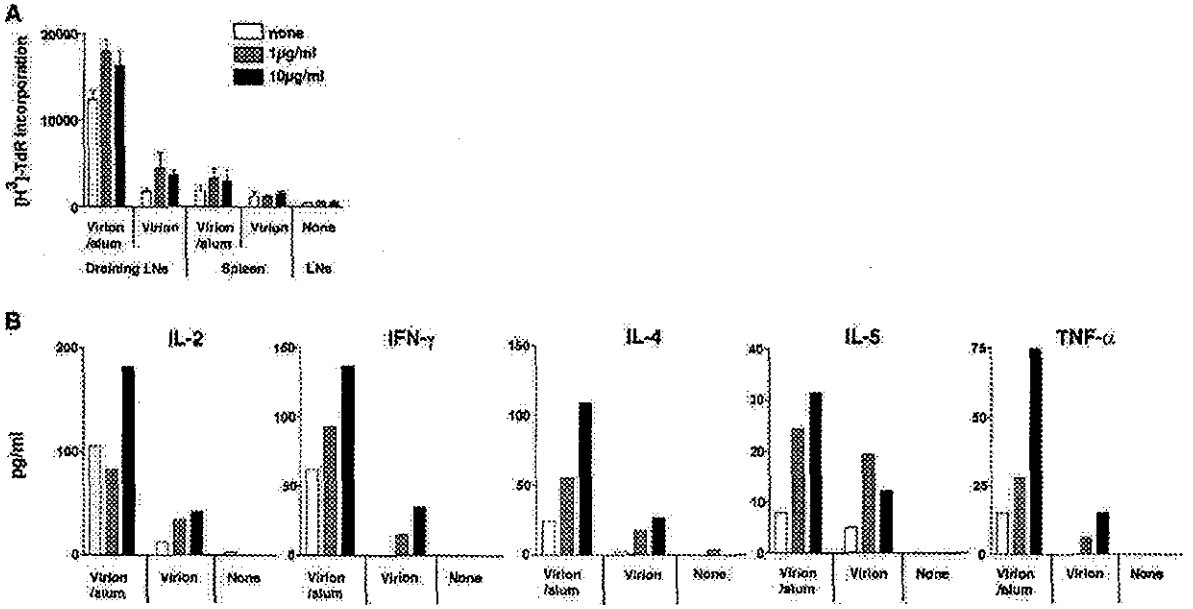

Fig. 5. *In vitro* responses of SARS-CoV-specific T cells taken from mice vaccinated with inactivated SARS-CoV. Mice were subcutaneously primed with 10 μg of UV-inactivated SARS-CoV virion, or virion with 2 mg of alum, or none, and then boosted with the same dose in their footpads at 7 weeks after priming. Draining lymph nodes and spleens were isolated at 1 week after boost and stimulated with T-cell depleted splenocytes that had been pulsed with the indicated concentration of UV-inactivated SARS-CoV virion. These cells were cultured for 2–4 days and [^{3}H]thymidine was added 8 h prior to the harvest. The peak response on day 4 after cultivation is shown in (A). (B) Culture supernatant was collected at day 2–4 post cultivation and the level of IL-2, IFN-γ, IL-4, IL-5 and TNF-α was determined by CBA kit. The maximum cytokine production at day 4 is shown. Results are representative of two separate experiments.

structures such as hepatitis B virus surface antigen-based, HIV-1 Gag-based and Ty virus-like particles have been shown to elicit humoral as well as cellular immune responses (19), these particulates probably have comparable dimensions and structures to the pathogens that are targeted for uptake by APCs to facilitate the induction of potent immune responses. The antibodies elicited in mice vaccinated by the current protocol with or without adjuvant recognized both the S and N proteins of SARS-CoV and were able to neutralize the infection of virus to Vero E6 cells. However, serum anti-SARS-CoV IgA antibody was not detectable, probably owing to the route of vaccination. In addition, the present vaccination protocol caused T cell response at the regional lymph nodes, although it did not allow for the induction of a sufficient cellular immune response systemically.

We show here the potentiality of subcutaneous injection of inactivated virion with alum, which is utilized for most of current human vaccinations. Alum has been used as an adjuvant for vaccines such as diphtheria, pertussis and tetanus, and these vaccines have a long safety record for human use (20). We observed that the addition of alum to the vaccine formula resulted in a large augmentation of serum IgG_1 production, but not IgG_{2a} production. The level of IgG_1 in alum-vaccinated mice reached a level similar to that found in hyper-immunized mice, which were subcutaneously injected with 5 μg of inactivated virion emulsified with a complete Freund adjuvant, followed by consecutive three-times intravenous boosters with 2 μg of virion. Alum is known to selectively stimulate an IgG_1 dominant, type 2 immune response [reviewed in (21)]. Activation of complement by alum could contribute to the type 2-biased immune response partly via an inhibition of IL-12 production. Interestingly, a quite recent report demonstrated that an alum-induced $Gr1^+$ myeloid cell population produced IL-4 and activated B-cells (22).

There are various diseases associated with animal coronavirus infection. The clinical manifestations of the disease and the correlates of protection with immunity have been studied extensively in these animal coronavirus infections [reviewed in (7)]. Although antibodies and T cells may play a role in exacerbating the pathology in some animal coronavirus infections (23,24), both humoral and cellular immune responses are known to contribute to protection against coronavirus infection. In murine hepatitis virus, a Group 2 coronavirus, the mortality of susceptible mice was partially prevented by the transfer of immune serum containing neutralizing antibody prior to challenge (25). Recently, Zhi-yong *et al.* reported in the murine acute infection model that the neutralizing antibody elicited by vaccination of DNA encoding S was protective, but cellular components of vaccinated mice were not required for the inhibition of viral replication (26). Because a twice parenteral administration of inactivated virion with alum induced a high level of antibodies that are able to neutralize SARS-CoV, this vaccination protocol may have a certain effect on the protection of humans from SARS-CoV infection.

We observed that two successive inoculations with inactivated virus at 7 week intervals generated SARS-CoV-specific

T cells. These cells were restimulated with the irradiated virus *in vitro*, but their response was low in terms of the level of proliferation and production of INF-γ and IL-2. However, irrespective of vaccination protocols with or without alum adjuvant, virus-primed T cells of vaccinated animals were capable of producing IL-4 at high levels upon *in vitro* stimulation, comparable to other reports for a variety of vaccination studies (27,28). This outlook seems compatible with the idea that the present vaccine protocol may tend to select T-cell subsets with Th2 phenotype. However, it remains to be elucidated whether such T cells may exhibit serological memory phenotype and persist in the immune system after vaccination as long as memory B cells, which may persist more than 180 days post vaccination. In addition, further analysis is needed to clarify whether T cell response is a crucial factor for long-term protection against SARS-CoV infections.

Efforts to develop a SARS-CoV vaccine have been carried out by many profitable or non-profitable organizations in various ways. For example, it has recently been reported that the combination of adenovirus vector expressing SARS-S, -M or -N protein elicited a neutralizing capacity in serum and N-specific T-cell response in rhesus macaques (29). However, it is still uncertain whether or not the immunity against only these components of SARS-CoV is sufficient for virus protection. SARS-CoV tends to cause replication errors, which may allow the virus to escape the host-immune response and result in a seasonal outbreak. From this point of view, it resembles influenza virus. In influenza virus, inactivated HA vaccine showed incomplete protection but had a certain efficacy and safety record for a long period of time. Indeed, this approach has been used in the veterinary field, such as with the bovine coronavirus (30) and canine coronavirus (31). These advantages make a whole killed virion a prime candidate for a SARS vaccine, even if it may not have the best protective ability.

Unfortunately, no information is available so far on the immune correlates of protection against human coronaviruses, including SARS-CoV. In consideration that SARS-CoV transmission occurs by direct contact with droplets or by the fecal oral route, mucosal secretary IgA in both the lower respiratory tract and digestive tract seem to be crucially important. Failure to induce IgA-type antibodies in a current systemic vaccination method should be improved. Notably, IgA antibodies were detectable in the sera and bronchoalveolar lavage fluid obtained from mice hyper-immunized with UV-irradiated virus (data not shown). Therefore, if a non-toxic and more potent adjuvant becomes available for human use, the subcutaneous injection of inactivated virion would become an effective vaccination method to reduce the number of susceptible people.

In the future, it will be necessary to determine whether or not the inactivated whole virion vaccine possesses protective ability against SARS-CoV infection by the use of adequate animal models. Furthermore, whether the alum addition augmented the protection and the effective period of SARS-CoV virion vaccination should be addressed, because currently used inactivated influenza virus whole virion vaccine is significantly effective without any adjuvant. Meanwhile, we also need to develop a potent adjuvant for induction of a much stronger mucosal immunity, in addition to evaluating available methods of virion inactivation.

Acknowledgements

We thank Ms R. Ishida, Ms Y. Kaburagi and Mr Y. Kimishima for their excellent technical help. This work was supported by a grant from the Ministry of Public Health and Labor of Japan.

Abbreviations

ACE2	angiotensin-converting enzyme 2
ASC	antibody-secreting cell
E	envelope
M	membrane
N	nucleocapsid protein
SARS	severe acute respiratory syndrome
SARS-CoV	SARS-associated coronavirus
S	spike protein

References

1 Drosten, C., Gunther, S., Preiser, W. *et al.* 2003. Identification of a novel coronavirus in patients with severe acute respiratory syndrome. *N. Engl. J. Med.* 348:1967.
2 Ksiazek, T. G., Erdman, D., Goldsmith, C. S. *et al.* 2003. A novel coronavirus associated with severe acute respiratory syndrome. *N. Engl. J. Med.* 348:1953.
3 Marra, M. A., Jones, S. J., Astell, C. R. *et al.* 2003. The genome sequence of the SARS-associated coronavirus. *Science* 300:1399.
4 Rota, P. A., Oberste, M. S., Monroe, S. S. *et al.* 2003. Characterization of a novel coronavirus associated with severe acute respiratory syndrome. *Science* 300:1394.
5 Holmes, K. V. and Enjuanes, L. 2003. Virology. The SARS coronavirus: a postgenomic era. *Science* 300:1377.
6 Liu, X., Shi, Y., Li, P., Li, L., Yi, Y., Ma, Q. and Cao, C. 2004. Profile of antibodies to the nucleocapsid protein of the severe acute respiratory syndrome (SARS)-associated coronavirus in probable SARS patients. *Clin. Diagn. Lab. Immunol.* 11:227.
7 De Groot, A. S. 2003. How the SARS vaccine effort can learn from HIV—speeding towards the future, learning from the past. *Vaccine* 21:4095.
8 Li, W., Moore, M. J., Vasilieva, N. *et al.* 2003. Angiotensin-converting enzyme 2 is a functional receptor for the SARS coronavirus. *Nature* 426:450.
9 Collins, R. A., Knobler, R. L., Powell, H. and Buchmeier, M. J. 1982. Monoclonal antibodies to murine hepatitis virus-4 (strain JHM) define the viral glycoprotein responsible for attachment and cell–cell fusion. *Virology* 119:358.
10 Fleming, J. O., Stohlman, S. A., Harmon, R. C., Lai, M. M., Frelinger, J. A. and Weiner, L. P.1983. Antigenic relationship of murine coronaviruses: analysis using monoclonal antibodies to JHM (MHV-4) virus. *Virology* 131:296.
11 Jackwood, M. W. and Hilt, D. A. 1995. *Production and immunogenicity of multiple antigenic peptide (MAP) constructs derived from the S1 glycoprotein of infectious bronchitis virus (IBV). Adv. Exp. Med. Biol.* 380:213.
12 Anton, I. M., Gonzalez, S., Bullido, M. J., Corsin, M., Risco, C., Langeveld, J. P. and Enjuanes, L. 1996. Cooperation between transmissible gastroenteritis coronavirus (TGEV) structural proteins in the *in vitro* induction of virus-specific antibodies. *Virus Res.* 46:111.
13 Ishii, K., Ueda, Y., Matsuo, K. *et al.* 2002. Structural analysis of vaccinia virus DIs strain: application as a new replication-deficient viral vector. *Virology* 302:433.
14 Storch, G. A. 2001. Diagnostic virology. In Knipe, D. M., Howley, P. M., ed., *Fields Virology*, 4th edn. Lippincott Williams & Wilkins, Philadelphia, PA. pp. 493–531.
15 Benner, R., Hijmans, W. and Haaijman, J. J. 1981. The bone marrow: the major source of serum immunoglobulins, but still a neglected site of antibody formation. *Clin. Exp. Immunol.* 46:1.
16 Slifka, M. K., Matloubian, M. and Ahmed, R. 1995. Bone marrow is a major site of long-term antibody production after acute viral infection. *J. Virol.* 69:1895.
17 Schmidt, O. W. and Kenny, G. E. 1982. Polypeptides and functions of antigens from human coronaviruses 229E and OC43. *Infect. Immun.* 35:515.

18 Xiao, X., Chakraborti, S., Dimitrov, A. S., Gramatikoff, K. and Dimitrov, D. S. 2003. The SARS-CoV S glycoprotein: expression and functional characterization. *Biochem. Biophys. Res. Commun.* 312:1159.
19 Singh, M. and O'Hagan, D. 1999. Advances in vaccine adjuvants. *Nat. Biotechnol.* 17:1075.
20 Clements, C. J. and Griffiths, E. 2002. The global impact of vaccines containing aluminium adjuvants. *Vaccine* 20 (Suppl. 3): S24.
21 HogenEsch, H. 2002. Mechanisms of stimulation of the immune response by aluminum adjuvants. *Vaccine* 20 (Suppl. 3): S34.
22 Jordan, M. B., Mills, D. M., Kappler, J., Marrack, P. and Cambier, J. C. 2004. Promotion of B cell immune responses via an alum-induced myeloid cell population. *Science* 304:1808.
23 Weiss, R. C. and Scott, F. W. 1981. Antibody-mediated enhancement of disease in feline infectious peritonitis: comparisons with dengue hemorrhagic fever. *Comp. Immunol. Microbiol. Infect. Dis.* 4:175.
24 Wu, G. F., Dandekar, A. A., Pewe, L. and Perlman, S. 2001. The role of CD4 and CD8 T cells in MHV-JHM-induced demyelination. *Adv. Exp. Med. Biol.* 494:341.
25 Pope, M., Chung, S. W., Mosmann, T., Leibowitz, J. L., Gorczynski, R. M. and Levy, G. A. 1996. Resistance of naive mice to murine hepatitis virus strain 3 requires development of a Th1, but not a Th2, response, whereas pre-existing antibody partially protects against primary infection. *J. Immunol.* 156:3342.
26 Yang, Z. Y., Kong, W. P., Huang, Y., Roberts, A., Murphy, B. R., Subbarao, K. and Nabel, G. J. 2004. A DNA vaccine induces SARS coronavirus neutralization and protective immunity in mice. *Nature* 428:561.
27 Mazumdar, T., Anam, K. and Ali N. 2004. A mixed Th1/Th2 response elicited by a liposomal formation of *Leishmania* vaccine instructs Th1 responses and resistance to *Leishmania donovani* in susceptible BALB/c mice. *Vaccine* 22:1162.
28 Nicollier-Jamot, B., Ogier, A., Piroth, L., Pothier, P. and Kohli, E. 2004. Recombinant virus-like particles of a norovirus (genogroup II strain) administered intranasally and orally with mucosal adjuvants LT and LT(R192G) in BALB/c mice induce specific humoral and cellular Th1/Th2-like immune responses. *Vaccine* 22:1079.
29 Gao, W., Tamin, A., Soloff, A., D'Aiuto, L., Nwanegbo, E., Robbins, P. D., Bellini, W. J., Barratt-Boyes, S. and Gambotto, A. 2003. Effects of a SARS-associated coronavirus vaccine in monkeys. *Lancet* 362:1895.
30 Takamura, K., Matsumoto, Y. and Shimizu, Y. 2002. Field study of bovine coronavirus vaccine enriched with hemagglutinating antigen for winter dysentery in dairy cows. *Can. J. Vet. Res.* 66:278.
31 Pratelli, A., Tinelli, A., Decaro, N., Cirone, F., Elia, G., Roperto, S., Tempesta, M. and Buonavoglia, C. 2003. Efficacy of an inactivated canine coronavirus vaccine in pups. *New Microbiol.* 26:151.

Jpn. J. Infect. Dis., 57, 55-57, 2004

Short Communication

Possible Horizontal Transmission of Crimean-Congo Hemorrhagic Fever Virus from a Mother to Her Child

Masayuki Saijo, Qing Tang[1], Bawudong Shimayi[2], Lei Han[1], Yuzhen Zhang[3], Muer Asiguma[3], Dong Tianshu[3], Akihiko Maeda, Ichiro Kurane and Shigeru Morikawa*

Special Pathogens Laboratory, Department of Virology I, National Institute of Infectious Diseases, Tokyo 208-0011, Japan,
[1]Second Division of Viral Hemorrhagic Fever, Institute of Infectious Disease Control and Prevention, Chinese Center for Disease Control and Prevention, Beijing 102206,
[2]Bachu County Center for Disease Prevention and Control, the Xinjiang Autonomous Region and
[3]Bachu People's Hospital, the Xinjiang Uygur Autonomous Region, P. R. China

(Received December 5, 2003. Accepted February 9, 2004)

SUMMARY: The case of a child with Crimean-Congo hemorrhagic fever (CCHF) presumably infected with CCHF virus from her 27-year-old mother is described. The mother with CCHF was treated with ribavirin and did not present with any symptoms of obvious hemorrhage. The child developed fever on the 5th day after the mother's onset. The partial virus genome was amplified by RT-PCR, and nested PCR from the child and the genome sequence were identical to that from the mother, indicating possible transmission of the virus from mother to child. This case indicates the importance of preventive measures for in-house outbreaks of CCHF.

Crimean-Congo hemorrhagic fever (CCHF) virus (CCHFV), a tick-borne virus distributed across Africa, Eastern Europe, the Middle East, and Asia, causes illness in humans and has a high fatality rate of up to 30% (1). Humans are usually infected with the virus through the bite of a tick (genus, *Hyalomma*) or by close contact with freshly slaughtered meat, or blood from viremic animals such as sheep, cattle, and goats (1). CCHF outbreaks have also occurred as nosocomial infections in several instances (2-5). In a review article by Hoogstraal (6), several cases of human-to-human infection of CCHF in households were described, indicating the importance of this infection route in CCHF outbreaks. However, the impact of human-to-human transmission of CCHFV in a household has not been studied with virological analysis, although in-house outbreaks of CCHF are considered to be relatively frequent, beyond expectations.

A 27-year-old female, who lived in a village in the Western part of the Xinjiang Uygur Autonomous Region, P. R. China, presented with fever, backache, headache, flushed face and general malaise without obvious hemorrhagic symptoms, and was transferred to a local hospital. She was diagnosed as having CCHF based on the epidemiology of CCHF in the area, and was hospitalized and treated with a 0.8 g/dose of ribavirin by drip infusion, twice daily for 7 days. Five days after the onset of the symptoms, her 4-year-old daughter also presented with high fever. She was clinically diagnosed as having CCHF, and was treated with intravenous administration of a 0.4 g/dose of ribavirin through drip infusion, twice a day for 7 days. No other proximate households showed any symptoms such as fever, arthralgia, and bleeding around that time. Both these patients lived in close contact with ticks, though neither recalled being bitten by one. Neither patient developed hemorrhagic manifestations. They recovered without any consequences.

Taking the day on which the fever first appeared as day 1, blood specimens were collected on days 3 and 11 from the mother and on days 3 and 8 from the daughter (Table 1). Serum samples were carefully separated under strict precautions, wearing a mask, protective glasses, double gloves, and a gown. RNA was extracted from serum samples using a High Pure Viral RNA Kit (Roche Diagnostics GmbH, Mannheim, Germany), according to the manufacturer's instructions. The reverse-transcription polymerase chain reaction (RT-PCR) and nested PCR was performed for amplification of a portion of the S-RNA segment according to the previous report (7) with some modifications (8). Serum samples were heat-inactivated at 56°C for 1 h for serological assays.

CCHFV immunoglobulin G (IgG) antibodies were detected by recombinant CCHFV nucleoprotein (CCHFV rNP)-based IgG enzyme-linked immunosorbent assay (ELISA) as described previously (9). CCHFV IgM antibodies were also detected by IgM-capture ELISA format using purified CCHFV rNP as an antigen (8). The cutoff optical density values for both ELISA tests were set at 0.200 (8,9).

The CCHFV genome was successfully amplified from the samples taken from the mother on days 3 and 11 and from the daughter on day 3 (Table 1). The daughter's serum collected on day 8 showed a positive reaction in the IgM-capture ELISA. The serum sample collected from the mother on day 11 also showed a positive reaction in the IgM-capture ELISA. On the other hand, a significant IgG response was demonstrated in the daughter but not in the mother (Table 1). The 262-base viral genome fragments, which were amplified in the sera collected from the mother and the child, respectively, were sequenced using ABI PRISM 310 Genetic Analyzer (Applied Biosystems, Foster City, Calif., USA). The nucleotide sequences of these viral genomes were the same (Accession No. AB102852 and AB102853 in DNA Data Bank of Japan). Furthermore, the sequence was confirmed to be identical to

*Corresponding author: Mailing address: Special Pathogens Laboratory, Department of Virology I, National Institute of Infectious Diseases, Gakuen 4-7-1, Musashimurayama, Tokyo 208-0011, Japan. Tel: +81-42-561-0771 ext. 791, Fax: +81-42-561-2039, E-mail: morikawa@nih.go.jp

Table 1. Results of RT-PCR, IgG ELISA, and IgM-capture ELISA

Virological tests	Serum samples collected from				
		Mother		Daughter	
	on day	3	11	3	8
RT-PCR		±[1]	+	+	−[1]
IgG ELISA (OD_{405})		−(0.071[2])	−(0.059)	−(0.059)	+(0.310)
IgM-capture ELISA (OD_{405})		−(0.015[3])	+(0.216)	−(0.021)	+(1.433)

[1]: + and - indicate positive and negative results, respectively.
[2, 3]: The OD_{405} values in IgG ELISA and IgM-capture ELISA were measured at the dilution level of 1:400 and 1:100, respectively.

that of CCHFV Chinese strain 66019 (Accession No. AJ101648 in National Center for Biotechnology Information). Although the data are not shown here, the CCHF outbreak in the region of residency in 2002 was caused by multiple strains of CCHFV. The partial viral genomes amplified from three patients, including the mother and her daughter, out of 6 patients from whom CCHFV genomes were amplified, were identical. This result strongly suggests that the pair were infected with the same strain of CCHFV from the same source or that the daughter was infected by her mother.

The incubation period of CCHF is 4-7 days (1). The interval between the onset of the mother and that of the child was 5 days. If both of them were infected with CCHFV simultaneously from the same source on the same occasion, the expected incubation time for the mother and her daughter would be 4-7 and 9-12 days, respectively. The expected incubation time of 9-12 days in the daughter is too long, suggesting that she was not infected with CCHFV at the same time her mother was. Therefore, it is quite likely that she was infected by her mother. However, we must not exclude the possibility that they were infected with CCHFV from the same source but on different occasions.

The mother did not show any symptoms of bleeding; therefore, if the daughter was infected by her mother, the daughter was infected through close contact with visually non-bloody bodily fluids secreted from the mother such as saliva, respiratory secretions, and/or urine. It is also possible that traces of blood were present in the mother's bodily fluids. This case of possible mother-to-child horizontal transmission of CCHFV indicates the importance of preventive measures in a household, even in cases without any hemorrhagic manifestations. In order to prevent in-house outbreaks, it must be emphasized that the education of the residents in endemic areas concerning modes of CCHFV transmission, risk of infection, and preventive measures is essential. In addition, rapid and accurate diagnosis of CCHF is also necessary.

The present study indicates the necessity of preventive measures against transmission of CCHFV to caregivers such as family members and hospital staff. It must be stressed that not only blood but also other bodily fluids should be regarded as possible sources of human-to-human transmission.

These patients were treated with an intravenous administration of ribavirin with favorable outcomes, as reported previously (8). The efficacy of ribavirin should be studied as a treatment of CCHF in the future.

In summary, we reported a pediatric case of CCHF, confirmed by virological studies, in which a child was possibly infected by her mother.

ACKNOWLEDGMENTS

The blood samples used in the study were drawn under the condition of informed consent. The study was approved by the ethical committee for biomedical science of the National Institute of Infectious Diseases, Tokyo, Japan.

We thank Professor C. J. Peters (The University of Texas Medical Branch) for helpful and critical comments. We acknowledge Dr. F. Li, Director of the AIDS Preventive and Control Center, the Xinjiang Epidemic Prevention Station, Urumqi, the Xinjiang Uygur Autonomous Region, and his colleagues for their excellent technical assistance with the work.

This study was partly supported by grants from the Ministry of Health, Labour and Welfare, Japan.

REFERENCES

1. Nichol, S. T. (2001): Bunyaviruses. p. 1603-1633. *In* Knipe, D. M. and Howley, P. M. (eds.), Fields Virology. vol. II. 4th ed. Lippincott Williams & Wilkins, Philadelphia.
2. Suleiman, M. N., Muscat-Baron, J. M., Harries, J. R., Satti, A. G., Platt, G. S., Bowen, E. T. and Simpson, D. I. (1980): Congo/Crimean hemorrhagic fever in Dubai. An outbreak at the Rashid Hospital. Lancet, ii, 939-941.
3. van Eeden, P. J., Joubert, J. R., van de Wal, B. W., King, J. B., de Kock, A. and Groenewald, J. H. (1985): A nosocomial outbreak of Crimean-Congo haemorrhagic fever at Tygerberg Hospital. Part I. Clinical features. S. Afr. Med. J., 68, 711-717.
4. Fisher-Hoch, S. P., Khan, A. J., Rehman, S., Rehman, S., Mirza, S., Khurshid, M. and McCormick, J. B. (1995): Crimean Congo-haemorrhagic fever treated with oral ribavirin. Lancet, 346, 472-475.
5. Papa, A., Bozovi, B., Pavlidou, V., Papadimitriou, E., Pelemis, M. and Antoniadis, A. (2002): Genetic detection and isolation of Crimean-Congo hemorrhagic fever virus, Kosovo, Yugoslavia. Emerg. Infect. Dis., 8, 852-854.
6. Hoogstraal, H. (1979): The epidemiology of tick-borne Crimean-Congo hemorrhagic fever in Asia, Europe, and Africa. J. Med. Entomol., 15, 307-417.
7. Rodriguez, L. L., Maupin, G. O., Ksiazek, T. G., Rollin, P. E., Khan, A. S., Schwarz, T. F., Lofts, R. S., Smith, J. F., Noor, A. M., Peters, C. J. and Nichol, S. T. (1997): Molecular investigation of a multisource outbreak of Crimean-Congo hemorrhagic fever in the United Arab Emirates. Am. J. Trop. Med. Hyg., 57, 512-518.
8. Tang, Q., Saijo, M., Zhang, Y., Asiguma, M., Tianshu, D., Han, L., Shimayi, B., Maeda, A., Kurane, I. and Morikawa,

S. (2003): A patient with Crimean-Congo hemorrhagic fever diagnosed with recombinant nucleoprotein-based antibody detection systems. Clin. Diagn. Lab. Immunol., 10, 489-491.
9. Saijo, M., Tang, Q., Niikura, M., Maeda, A., Ikegami, T., Prehaud, C. and Morikawa, S. (2002): Recombinant nucleoprotein based enzyme-linked immunosorbent assay for detection of immunoglobulin G to Crimean-Congo hemorrhagic fever virus. J. Clin. Microbiol., 40, 1587-1591.

Journal of Medical Virology 75:295–299 (2005)

Recombinant Nucleoprotein-Based Serological Diagnosis of Crimean–Congo Hemorrhagic Fever Virus Infections

Masayuki Saijo,[1]* Qing Tang,[2] Bawudong Shimayi,[3] Lei Han,[2] Yuzhen Zhang,[4] Muer Asiguma,[4] Dong Tianshu,[4] Akihiko Maeda,[1] Ichiro Kurane,[1] and Shigeru Morikawa[1]

[1]*Department of Virology 1, Special Pathogens Laboratory, National Institute of Infectious Diseases, Musashimurayama, Tokyo, Japan*
[2]*Second Division of Viral Hemorrhagic Fever, Institute of Infectious Diseases Control and Prevention, Chinese Center for Disease Control and Prevention, Beijing, China*
[3]*Bachu County Center for Disease Prevention and Control, Kashi District, Xinjiang Autonomous Region, China*
[4]*Xinjiang Bachu County People's Hospital, Bachu county, Kashi District, the Xinjiang Uygur Autonomous Region, China*

An enzyme-linked immunosorbent assay (ELISA) using recombinant nucleoprotein (rNP) was reported for the detection of immunoglobulin G (IgG) antibodies to Crimean–Congo hemorrhagic fever (CCHF) virus (CCHFV). The immunoglobulin M (IgM)-capture ELISA was developed for the diagnosis of CCHFV infections, using CCHFV rNP as an antigen. These newly developed assays were applied to a study of a CCHF-outbreak and evaluated with sera collected from patients diagnosed as having CCHF by positive reverse transcription-polymerase chain reaction (RT-PCR) and by detection of IgG response. IgM antibodies to CCHFV were detected in 10 of the 13 patients. IgM antibodies to the rNP of CCHFV were detected by the CCHFV rNP-based IgM-capture ELISA in all 6 patients in whom IgG responses were demonstrated, while it was not detected in the 10 patients in whom IgG responses were not demonstrated. Furthermore, the IgM antibodies were detected in 6 of the 61 residents living a CCHF endemic area during the endemic season, while it was not detected in any of the 48 Japanese residents that had never visited the CCHF endemic area. It is concluded that this newly developed CCHFV rNP-based IgM-capture ELISA is a useful method for the diagnosis of CCHFV infections. ***J. Med. Virol. 75: 295–299, 2005.*** © 2004 Wiley-Liss, Inc.

KEY WORDS: Crimean–Congo hemorrhagic fever; CCHF; recombinant nucleoprotein; ELISA; RT-PCR; serological diagnosis

INTRODUCTION

Crimean–Congo hemorrhagic fever (CCHF) virus (CCHFV) is a member of the family Bunyaviridae, genus *Nairovirus* [Nichol, 2001]. CCHF is an acute viral hemorrhagic fever with a high mortality rate of up to 30% [Nichol, 2001]. Humans are infected with the virus by a tick (genus *Hyalomma*) bite or by close contact with freshly slaughtered meat or blood from viremic animals including sheep, cattle, and goats [Nichol, 2001]. CCHFV infections in humans have been reported in Africa, Eastern Europe, the Middle East, and Central and Southern Asia [Hoogstraal, 1979]. The actual number of patients with CCHF is believed to be far greater than that reported, because the disease usually occurs in remote areas. Noscomial outbreaks of CCHF are not rare [Burney et al., 1980; Suleiman et al., 1980; van Eeden et al., 1985; Fisher-Hoch et al., 1995; Papa et al., 2002].

Although there have been no reports of the efficacy of ribavirin therapy for CCHF as evaluated by a control-based study, ribavirin is known to inhibit the replication of CCHFV in vitro and in vivo [Huggins, 1989; Watts et al., 1989; Tignor and Hanham, 1993]. Furthermore, there have been several reports of patients with CCHF treated successfully with ribavirin [van de Wal et al., 1985; Fisher-Hoch et al., 1992; Papa et al., 2002; Tang et al., 2003]. Therefore, the rapid diagnosis of CCHF is important.

The study was performed under the approval of the ethical committee on medical research and human rights, National Institute of Infectious Diseases, Tokyo, Japan.

Grant sponsor: Ministry of Health, Labor, and Welfare of Japan (grant-in-aid).

*Correspondence to: Masayuki Saijo, Department of Virology 1, Special Pathogens Laboratory, National Institute of Infectious Diseases, 4-7-1 Gakuen, Musashimurayama, Tokyo 208-0011, Japan. E-mail: msaijo@nih.go.jp

Accepted 14 October 2004
DOI 10.1002/jmv.20270
Published online in Wiley InterScience (www.interscience.wiley.com)

The CCHFV recombinant nucleoprotein (rNP)-based enzyme-linked immunosorbent assay (ELISA) and immunofluorescent assay are effective for the detection of immunoglobulin G (IgG) antibodies to CCHFV [Saijo et al., 2002a; Saijo et al., 2002b]. Paired serum samples are required for diagnosis by IgG ELISA, because a significant rise in antibody titers must be demonstrated. Detection of immunoglobulin M (IgM) antibodies is another reliable procedure for the rapid diagnosis of CCHF. A patient who was diagnosed as having CCHF by detection of IgM and IgG antibodies using CCHFV rNP-based ELISAs was reported previously [Tang et al., 2003].

In the present study, a CCHFV rNP-based IgM-capture ELISA was evaluated for its efficacy in diagnosis of CCHF using sera collected from patients with acute CCHF confirmed by viral genome amplification with RT-PCR and/or by the detection of IgG responses with rNP-based IgG ELISA. The relationship of IgM and IgG responses determined by the CCHFV rNP-based ELISAs with viremia determined by RT-PCR was examined.

MATERIALS AND METHODS

Serum Samples

The western part of the Xinjiang Uygur Autonomous Region, China, is known to be the site of CCHF outbreaks [Yen et al., 1985; Saijo et al., 2002a; Saijo et al., 2002b; Qing et al., 2003; Tang et al., 2003]. Serum samples drawn from nine patients ("Panel A"), from whom the CCHFV genome was amplified by RT-PCR, in the region during the outbreak seasons in 2001 and 2002 were used. Subsequent serum samples were also collected from five of the nine patients approximately 1 week after the first samples were collected. The time of collection after onset was defined by taking the day on which fever first appeared as day 1. Although the exact days of blood sampling from the other four patients, from whom only the 1st blood samples were drawn, were unclear, these samples were collected within 10 days of onset; i.e., during the acute phase of CCHF. The samples from the two sampling times were designated as 1st and 2nd samples, respectively.

Apart from the nine patients, paired serum samples were collected from 14 individuals ("Panel B") in the same regions in the outbreak season. They were suspected as having CCHF or other viral infections based on clinical manifestations such as fever and joint pain.

There was a relatively large outbreak of CCHF in a small village in the area (data not shown). Serum samples were collected from 61 residents, "Panel C", living in the CCHF endemic area in June 2001, at which time the CCHF outbreak had nearly ended. The age of these residents ranged from 6 to 66 and the male to female ratio was 38:23.

Serum samples collected from 48 Japanese subjects, "Panel D", who had never visited the CCHF endemic area, were used as a control.

The sera used in the present study were collected under informed consent. In the case of unconscious patients and children less than 20 years of age, informed consent was obtained from their family members and parents, respectively.

Positive- and negative-control sera for IgG and IgM-capture ELISA were produced in a monkey (*Macaca fascicularis*) by immunization with the purified His-CCHFV rNP using Inject Alum™ (Pierce Biotechnology, Inc., Rockford, IL) [Saijo et al., 2002b] and were tested by each IgG ELISA and IgM-capture ELISA for verification.

CCHFV rNP-Based IgG ELISA and IgM-Capture ELISA

The CCHFV rNP was expressed as a fusion protein with a 6× His-tag on the N-terminus in the recombinant baculovirus system and was designated CCHFV rNP [Saijo et al., 2002b]. The IgG antibodies to CCHFV were detected by IgG ELISA using CCHFV rNP in the same way as described previously [Saijo et al., 2002b]. The CCHFV rNP-base IgM-capture ELISA was performed as previously reported [Tang et al., 2003].

Reverse Transcription-Polymerase Chain Reaction (RT-PCR)

The details of RT-PCR were also described in a previous paper [Tang et al., 2003].

RESULTS

Cut-Off Values of OD_{405} in IgG and IgM-Capture ELISA

Forty-eight serum samples collected from the "Panel D" subjects were tested as a negative control for the IgM-capture ELISA. The OD_{405}s at a dilution of 1:100 were between −0.17 and 0.15, and the average and standard deviation (SD) at that dilution were −0.008 and 0.071, respectively. The cut-off value, calculated as the average +3SD, was 0.205. Positive and negative results by the IgM-capture ELISA were judged on the basis of this cut-off value at a dilution of 1:100. This cut-off value was applied to the other dilution levels, 1:50, 1:200, and 1:400.

The average and SD values of the adjusted optical density (OD_{405}) at a dilution of 1:400 in the IgG ELISA were 0.069 and 0.039, respectively. Therefore, the cut-off value [average + 3× SD of "Panel D" sera] in the IgG ELISA format measured at a dilution of 1:400 was set at 0.186 in the study. This cut-off value was also applied to the other dilution levels, 1:100, 1:1,600, and 1:6,400.

IgM Responses Determined by IgM-Capture ELISA

The IgM antibody status to CCHFV rNP together with the results of RT-PCR and IgG ELISA are shown in Tables I and II. Positive IgM responses were demonstrated in six of the "Panel A" patients: two in the first

TABLE I. RT-PCR and IgG/IgM Responses to CCHFV rNP in the Serum Samples Drawn From Nine "Panel A" Patients With CCHF as Diagnosed by Positive RT-PCR

	Day(s) after onset, RT-PCR, IgM, and IgG ELISA							
	1st samples (collected within day 3)				2nd samples (collected between days 5 and 11)			
Patient ID	Day(s)[a]	RT-PCR[b]	IgM (OD_{405})[c]	IgG (OD_{405})[d]	Day(s)[a]	RT-PCR[b]	IgM (OD_{405})[c]	IgG (OD_{405})[d]
1	2	+	−(0.035)	−(0.071)	8	+	−(0.065)	−(0.059)
2	2	+	−(0.015)	−(0.071)	10	+	+(0.216)	−(0.058)
3	2	+	−(0.021)	−(0.059)	8	−	+(1.433)	−(0.160)
4[e]	1	+	−(0.020)	−(0.031)	5	−	+(2.711)	+(0.972)
5	3	+	−(0.000)	−(0.007)	11	−	+(1.227)	+(0.235)
6	UK[f]	+	−(0.060)	−(0.181)		ND[g]		
7	UK	+	−(0.016)	−(0.024)		ND		
8	UK	+	+(2.208)	−(0.023)		ND		
9	UK	+	+(0.860)	−(0.019)		ND		

[a]Day(s) after onset was defined by taking the day on which fever first appeared as day 1.
[b]"+" and "−" indicate positive and negative reactions in RT-PCR, respectively.
[c]"+" and "−" indicate positive and negative reactions in IgM-capture ELISA, respectively. The OD_{405} values at a dilution level of 1:100 are shown.
[d]"+" and "−" indicate positive and negative reactions in IgG ELISA, respectively. The OD_{405} values at a dilution level of 1:400 are shown.
[e]This case was reported in the previous report [Tang et al., 2003].
[f]"UK" indicates unknown.
[g]"ND" indicates not drawn.

set of samples and four in the second set of samples (Table I). Positive IgM responses were demonstrated in four of the five patients (Patients 1–5) from whom 2nd samples were collected, but no IgM responses were demonstrated in any of the five 1st samples from these patients (Table I). The IgM antibody to CCHFV was not detected in Patient 1 within 8 days from onset.

Of the nine patients, in whom the CCHFV genome was amplified, a significant rise in IgG antibody titer was demonstrated in two patients (Patients 4 and 5, Table I). Furthermore, a significant rise in IgG antibody titer was demonstrated in 4 individuals (Patients 10–13, Table II) of the 14 "Panel B" patients from whom a paired serum sample was collected. In summary, IgG responses defined as a positive significant rise in IgG antibody titer were demonstrated in six patients. The CCHFV rNP-based IgM-capture ELISA showed a positive reaction in the sera collected from all of the 6 patients (Table II), while it did not show a positive reaction in the sera collected from the other 10 "Panel B" patients, in whom IgG responses were not demonstrated.

Relationship of IgM, IgG Responses, and Viremia

The 1st and 2nd blood samples were drawn from five of the "Panel A" patients. The relationship between the time of sample collection after onset and antibody responses was evaluated in these patients.

IgM and IgG responses were demonstrated in four (80%) and two (40%) of the 2nd samples collected between day 5 and day 11, respectively, while no antibody responses were demonstrated in the 1st samples collected within 3 days after onset (Table I). On the other hand, all the 1st samples and two of the 2nd samples showed a positive reaction in RT-PCR (Table I).

Antibody Responses and Viremia

The relationship between the IgM responses and viremia was evaluated using the serum samples collected from the "Panel A" patients (Table I). Only 3 of the 11 RT-PCR-positive sera (27%) were positive by the IgM-capture ELISA, while all of the 3 RT-PCR-

TABLE II. IgM Responses to CCHFV rNP in Six Patients With CCHF Diagnosed by Positive IgG Responses Determined by CCHFV rNP-Based IgG ELISA

		OD_{405}s in IgM-capture (1:100), IgG ELISAs (1:100), and antibody titers					
		1st samples (within day 3)		2nd samples (days 8–14)		3rd samples (3–4 weeks from onset)	
Panel	Patient ID	IgM	IgG	IgM	IgG	IgM	IgG
A	4	0.020, <50	0.031, <100	2.711, ≥400	0.972, 1,600	ND[a]	ND
	5	0.000, <50	0.007, <100	1.227, ≥400	0.235, 400	ND	ND
B	10	0.159, <50	0.181, <100	0.359, 200	1.412, >6,400	ND	ND
	11	0.184, <50	0.128, <100	1.077, ≥400	1.408, >6,400	ND	ND
	12	ND	ND	3.129, ≥400	0.119, <100	2.761, ≥400	>3.500, ≥6,400
	13	ND	ND	3.147, ≥400	0.367, 400	2.669, ≥400	1.943, ≥6,400

[a]"ND" indicates not drawn.

negative samples were positive by the IgM-capture ELISA (Table I). In contrast, viral RNA was amplified by RT-PCR in all of the 11 IgM-negative and IgG-negative, in 3 of the 4 IgM-positive and IgG-negative samples, and in neither of the 2 IgM-positive and IgG-positive samples.

IgM and IgG Antibodies to CCHFV Among Residents in CCHF Endemic Area During the Outbreak Season

Of the 61 "Panel C" sera, 5 showed positive reactions by both IgM-capture and IgG ELISAs, 1 showed positive reaction by the IgM-capture ELISA only, 13 showed positive reactions by the IgG ELISA only, and the rest showed negative reactions by both IgM-capture and IgG ELISAs. Clinical manifestations in four of the six IgM-positive patients were available. All four patients had fever, headache, and backache. Two of the four had symptoms of nasal and gingival hemorrhage.

DISCUSSION

Patients with CCHF are usually seen in very remote areas and the number of patients with CCHF is relatively small. Patients with suspected CCHF do not always visit hospitals for treatment in CCHF endemic areas, because of economic difficulties and problems in gaining access to hospitals. Furthermore, the facilities at the hospitals in such remote areas are usually not adequate for virological testing or for storing serum samples. Therefore, virological testing of CCHF, and the collection and storage of blood samples are very difficult. Under such difficult conditions, the serum samples of patients with and without CCHF in one CCHF endemic area in the western part of the Xinjiang Uygur Autonomous Region were collected. The serum samples collected from 132 subjects including 13 CCHF-patients were used in the present study. Therefore, it is considered to be acceptable to draw conclusions regarding the efficacy of the rNP-based ELISA for serological diagnosis of and epidemiological study on CCHF by analyzing the data obtained in this study.

The patients with positive IgG responses, taken as the detection of a significant rise in IgG antibody titer determined by CCHFV rNP-based IgG ELISA, are considered to be CCHF-positive patients, because the IgG ELISA has been confirmed to have high sensitivity and specificity in detecting specific IgG antibodies to CCHFV [Saijo et al., 2002b]. Within this limited number of patients, the efficacy of the CCHFV rNP-based IgM ELISA in diagnosis of CCHF and the relationship between time after onset, antibody responses, and viremia were evaluated.

Six of the nine "Panel A" patients were confirmed to be IgM-positive by CCHFV rNP-based IgM-capture ELISA. The blood samples of the other three "Panel A" patients with IgM-negative result were collected within about 10 days after onset. If the blood had been collected a little later, IgM responses to CCHFV rNP would have been detected. IgM antibodies to CCHFV were detected in all the 6 patients with IgG responses to CCHFV (Table II), while no IgM antibodies were detected in any of the other 10 "Panel B" individuals in whom IgG responses not demonstrated. IgM antibodies to CCHFV were demonstrated in 6 of the 61 serum samples collected from the "Panel C" residents living in a CCHF endemic area during the outbreak season, while none of the Japanese sera showed a positive reaction in the IgM-capture ELISA. These data indicate that the IgM-capture ELISA using His-CCHFV rNP has high sensitivity and specificity in detecting IgM antibodies to CCHFV and that it is useful for the rapid and accurate diagnosis of CCHF. If the sensitivity and specificity are analyzed using the paired sera collected from 14 "Panel B" subjects composed of 4 CCHF-patients and 10 non-CCHF-patients, both the sensitivity and specificity would be considered to be 100%.

Although, further study is needed, the data in the present study suggest that the IgM antibodies to CCHFV become detectable within at least 2 weeks from onset. It was found that viremia was still present at the stage in which positive IgM responses but not IgG responses were observed and that the viremia was already eliminated at the stage in which positive IgG responses were observed. To increase the sensitivity in detecting viremia, nested RT-PCR was performed for serum samples. However, mononuclear phagocytes are one of the main targets of CCHFV infections [Burt et al., 1997]. Therefore, it is possible that the sensitivity of the nested RT-PCR for detection of the CCHFV genome increases when whole blood samples rather than serum samples are used.

The effectiveness of the newly developed CCHFV rNP-based IgM-capture ELISA for the diagnosis of CCHF should be compared with that of the already developed methods such as indirect immunofluorescence assay [Fisher-Hoch et al., 1992; Burt et al., 1998; Papa et al., 2002] and/or IgM-capture ELISA [Saluzzo and Le Guenno, 1987; Gonzalez et al., 1990; Chapman et al., 1991; Burt et al., 1994; Khan et al., 1997; Rodriguez et al., 1997; Schwarz et al., 1997] using authentic CCHFV antigens. However, CCHFV is regarded as a biosafety level-4 (BLS-4) pathogen in Japan, and viral antigen preparation is difficult. Therefore, the CCHFV rNP-based IgM-capture ELISA was not compared with IgM antibody detection systems using authentic viral antigens. The inability to produce authentic viral antigens was overcome by evaluating the CCHFV rNP-based IgM capture ELISA using the sera collected from patients with and without CCHF.

The main antigenic region in the NP of CCHFV (482 amino acid residues) was located on the central portion from amino acid positions 201 to 306 as reported previously [Saijo et al., 2002b]. The amino acid sequence of this region in NP (Chinese strain 8402) has 97%–100% homology to the other Chinese strains and 92%–96% homology to non-Chinese strains. Furthermore, the antibodies to CCHFV in Asian patients with CCHF were detected by the IgG ELISA using the recombinant NP of CCHFV strain IbAr 10200 (GenBank accession no.

U88410, data not shown). These results indicate that the IgM-capture ELISA using the CCHFV rNP of Chinese strain 8402 might be useful in detecting not only antibodies to CCHFV Chinese strains but also antibodies to strains in other regions.

As CCHFV is a BSL-4 pathogen, the preparation of the CCHFV antigen must be performed in a BSL-4 laboratory and this restriction makes the preparation of CCHF antigens difficult in institutes without a BLS-4 laboratory. It was demonstrated that the rNP-based IgM-capture ELISA offers a definite advantage in the diagnosis of and seroepidemiological study on CCHF. In summary, diagnosis by the combination of IgM-capture ELISA and RT-PCR is more sensitive, accurate, and reliable than that by either single method.

ACKNOWLEDGMENTS

We thank all the staff in the Xinjiang Bachu People's Hospital who contributed to the treatment of the patients. We also thank Dr. Li Fan, Director of the AIDS Prevention and Control Center, Xinjiang Epidemic Prevention Station, Urumqi, the Xinjiang Uygur Autonomous Region, and his colleagues. We are grateful to Ms. M. Ogata, Department of Virology 1, Special Pathogens Laboratory, National Institute of Infectious Diseases, Tokyo, Japan, and Ms. X. Zhao and Ms. X. Tao, the Second Division of Viral Hemorrhagic Fever, Institute of Infectious Disease Control and Prevention, Chinese Center for Disease Control and Prevention, for their excellent technical assistance in this work. The blood samples were drawn carefully from the patients in the hospital. The work dealing with the patients' blood samples was performed in a highly contained laboratory according to the regulations of the Institute of Infectious Disease Control and Prevention, Chinese Center for Disease Control and Prevention.

REFERENCES

Burney MI, Ghafoor A, Saleen M, Webb PA, Casals J. 1980. Nosocomial outbreak of viral hemorrhagic fever caused by Crimean hemorrhagic fever-Congo virus in Pakistan, January 1976. Am J Trop Med Hyg 29:941–947.

Burt FJ, Leman PA, Abbott JC, Swanepoel R. 1994. Serodiagnosis of Crimean–Congo haemorrhagic fever. Epidemiol Infect 113:551–562.

Burt FJ, Swanepoel R, Shieh W, Smith JF, Leman PA, Greer PW, Coffield LM, Rollin PE, Ksiazek TG, Peters CJ, Zaki SR. 1997. Immunohistochemical and in situ localization of Crimean–Congo hemorrhagic fever (CCHF) virus in human tissues and implications for CCHF pathogenesis. Arch Pathol Lab Med 121:839–846.

Burt FJ, Leman PA, Smith JF, Swanepoel R. 1998. The use of a reverse transcription-polymerase chain reaction for the detection of viral nucleic acid in the diagnosis of Crimean–Congo haemorrhagic fever. J Virol Methods 70:129–137.

Chapman LE, Wilson LM, Hall DB, LeGuenno B, Dykstra EA, Ba K, Fisher-Hoch SP. 1991. Risk factors for Crimean–Congo hemorrhagic fever in rural northern Senegal. J Infect Dis 164:686–692.

Fisher-Hoch SP, McCormick JB, Swanepoel R, Van Midderlkoop A, Harvey S, Kustner HG. 1992. Risk of human infections with Crimean–Congo hemorrhagic fever virus in a South African rural community. Am J Trop Med Hyg 47:337–345.

Fisher-Hoch SP, Khan JA, Rehman S, Mirza S, Khurshid M, McCormick JB. 1995. Crimean–Congo haemorrhagic fever treated with oral ribavirin. Lancet 346:472–475.

Gonzalez J, LeGuenno B, Guillaud M, Wilson ML. 1990. A fatal case of Crimean–Congo haemorrhagic fever in Mauritania: And serological evidence suggesting epidemic transmission. Trans Royal Trop Med Hyg 84:573–576.

Hoogstraal H. 1979. The epidemiology of tick-borne Crimean–Congo hemorrhagic fever in Asia, Europe, and Africa. J Med Entomol 15: 307–417.

Huggins JW. 1989. Prospects for treatment of viral hemorrhagic fevers with ribavirin, a broad spectrum antiviral drug. Rev Infect Dis ii:S750–S761.

Khan AS, Maupin GO, Rollin PE, Noor AM, Shurie HH, Shalabi AG, Wasef S, Haddad YM, Sadek R, Ijaz K, Peters CJ, Ksiazek TG. 1997. An outbreak of Crimean–Congo hemorrhagic fever in the United Arab Emirates, 1994–1995. Am J Trop Med Hyg 57:519–525.

Nichol ST. 2001. Bunyaviruses. In: Knipe DM, Howley P, editors. Fields virology, 4th ed. Philadelphia, PA: Lippincott-Raven, pp 1603–1633.

Papa A, Ma B, Kouidou S, Tang Q, Hang C, Antoniadis A. 2002. Genetic characterization of the MRNA segment of Crimean–Congo hemorrhagic fever virus strains, China. Emerg Infect Dis 8:50–53.

Qing T, Saijo M, Lei H, Maeda A, Ikegami T, Xinjung W, Kurane I, Morikawa S. 2003. Detection of immunoglobulin G to Crimean–Congo hemorrhagic fever virus in sheep sera by nucleoprotein-based enzyme-linked immunosorbent and immunofluorescence assays. J Virol Methods 108:111–116.

Rodriguez LL, Maupin GO, Ksiazek TG, Rollin PE, Khan AS, Schwarz TF, Lofts RS, Smith JF, Noor AM, Peters CJ, Nichol ST. 1997. Molecular investigation of a multisource outbreak of Crimean–Congo hemorrhagic fever in the United Arab Emirates. Am J Trop Med Hyg 57:512–518.

Saijo M, Qing T, Niikura M, Maeda A, Ikegami T, Sakai K, Prehaud C, Kurane I, Morikawa S. 2002a. Immunofluorescence technique using HeLa cells expressing recombinant nucleoprotein for detection of immunoglobulin G antibodies to Crimean–Congo hemorrhagic fever virus. J Clin Microbiol 40:372–375.

Saijo M, Qing T, Niikura M, Maeda A, Ikegami T, Prehaud C, Kurane I, Morikawa S. 2002b. Recombinant nucleoprotein based enzyme-linked immunosorbent assay for detection of immunoglobulin G to Crimean–Congo hemorrhagic fever virus. J Clin Microbiol 40: 1587–1591.

Saluzzo J, Le Guenno B. 1987. Rapid diagnosis of human Crimean–Congo hemorrhagic fever and detection of the virus in naturally infected ticks. J Clin Mircobiol 25:922–924.

Schwarz TF, Nsanze H, Ameen AM. 1997. Clinical features of Crimean–Congo haemorrhagic fever in the United Arab Emirates. Infection 25:364–367.

Suleiman MN, Muscat-Baron JM, Harries JR, Satti AG, Platt GS, Bowen ET, Simpson DI. 1980. Congo/Crimean haemorrhagic fever in Dubai. An outbreak at the Rashid Hospital. Lancet ii:939–941.

Tang Q, Saijo M, Yuzhen Y, Asiguma M, Tianshu D, Han L, Shimayi B, Maeda A, Kurane I, Morikawa S. 2003. A patient with Crimean–Congo hemorrhagic fever serologically diagnosed by recombinant nucleoprotein-based antibody detection systems. Clin Diagn Lab Immunol 10:489–491.

Tignor GH, Hanham CA. 1993. Ribavirin efficacy in an in vivo model of Crimean–Congo hemorrhagic fever virus (CCHF) infection. Antiviral Res 22:309–325.

van de Wal BW, Joubert JR, van Eeden PJ, King JB. 1985. A nosocomial outbreak of Crimean–Congo haemorrhagic fever at Tygerberg Hospital. Part IV. Preventive and prophylactic measures. S Afr Med J 68:729–732.

van Eeden PJ, Joubert JR, van de Wal BW, King JL, de Kock A, Groenewald JH. 1985. A nosocomial outbreak of viral hemorrhagic fever caused by Crimean–Congo haemorrhagic fever at Tygerberg Hospital. Part I. Clinical features. S Afr Med J 68:711–717.

Watts DM, Ussery MA, Nash D, Peters CJ. 1989. Inhibition of Crimean–Congo hemorrhagic fever viral infectivity yields in vitro by ribavirin. Am J Trop Med Hyg 41:581–585.

Yen YC, Kong LX, Lee L, Zhang YQ, Li F, Cai BJ, Gao SY. 1985. Characteristics of Crimean–Congo hemorrhagic fever virus (Xinjiang strain) in China. Am J Trop Med Hyg 34:1179–1182.

Available online at www.sciencedirect.com
SCIENCE DIRECT®
ELSEVIER
Biochemical and Biophysical Research Communications 319 (2004) 1228–1234
BBRC
www.elsevier.com/locate/ybbrc

Phosphorylation of p38 MAPK and its downstream targets in SARS coronavirus-infected cells

Tetsuya Mizutani,* Shuetsu Fukushi, Masayuki Saijo, Ichiro Kurane, and Shigeru Morikawa

Special Pathogens Laboratory, Department of Virology 1, National Institute of Infectious Diseases, Gakuen 4-7-1, Musashimurayama, Tokyo 208-0011, Japan

Received 3 March 2004
Available online 7 June 2004

Abstract

Severe acute respiratory syndrome (SARS) has become a global public health emergency. Understanding the molecular mechanisms of SARS-induced cytopathic effects (CPEs) is a rational approach for the prevention of SARS, and an understanding of the cellular stress responses induced by viral infection is important for understanding the CPEs. Polyclonal antibodies, which recognized nucleocapsid (N) and membrane (M) proteins, detected viral N and M proteins in virus-infected Vero E6 cells at least 6 and 12 h post-infection (h.p.i.), respectively. Furthermore, detection of DNA ladder and cleaved caspase-3 in the virus-infected cells at 24 h.p.i. indicated that SARS-CoV infection induced apoptotic cell death. Phosphorylation of p38 MAPK was significantly up-regulated at 18 h.p.i. in SARS-CoV-infected cells. The downstream targets of p38 MAPK, MAPKAPK-2, HSP-27, CREB, and eIF4E were phosphorylated in virus-infected cells. The p38 MAPK inhibitor, SB203580, inhibited effectively phosphorylation of HSP-27, CREB, and eIF4E in SARS-CoV-infected cells. However, viral protein synthesis was not affected by treatment of SB203580.

Severe acute respiratory syndrome coronavirus (SARS-CoV) is the etiological agent responsible for the outbreak of SARS, an extremely severe disease that has spread to many countries throughout the world. In the period from February to June 2003, 32 countries were affected by SARS. SARS-CoV is a positive-strand RNA virus, and its genome is composed of about 29,700 nucleotides. The genomic organization of SARS-CoV is that of a typical coronavirus, and sequentially contains genes encoding polymerase (and polymerase-related proteins), spike, envelope, membrane (M), and nucleocapsid (N) proteins. Three groups of coronaviruses were known prior to SARS, while phylogenic analysis indicated SARS-CoV to be a member of a fourth group [1,2]. A vaccine is currently under development and there is no efficacious therapy for SARS.

Mitogen-activated protein kinases (MAPKs) are signal transducers that respond to extracellular stimulation by cytokines, growth factors, viral infection, and stress, and in turn regulate cell differentiation, proliferation, survival, and apoptosis [3–6]. In particular, p38 MAPK is strongly activated by stress and inflammatory cytokines. In the case of mouse hepatitis virus (MHV), a prototype coronavirus, virus-infected cells showed induction of p38 MAPK [7]. The SARS-CoV N protein has been reported to be involved in the regulation of cellular signaling pathways [8]. The levels of transcription factors binding to promoter sequences of c-Fos, ATF-2, CREB-1, and Fos B, which are related to AP-1, were increased by expression of N protein. However, there have been no previous reports regarding activation of signaling pathways by infection with SARS-CoV. In addition, no information is available regarding the molecular mechanisms of the cytopathic effects of SARS-CoV-infection. In the present study, we demonstrated that infection of Vero E6 cells by SARS-CoV induced apoptotic cell death and that p38 MAPK and its downstream targets were phosphorylated during viral replication. Understanding the mechanisms of p38

* Corresponding author. Fax: +81-42-565-3315.
E-mail address: tmizutan@nih.go.jp (T. Mizutani).

0006-291X/$ - see front matter © 2004 Elsevier Inc. All rights reserved.
doi:10.1016/j.bbrc.2004.05.107